

1 **Reactive uptake of ozone at simulated leaf surfaces: implications for ‘non-stomatal’**
2 **ozone flux.**

3
4 J. Neil Cape^{1*}, Richard Hamilton^{1,2} and Mathew R. Heal²

5
6 ¹Centre for Ecology & Hydrology, Bush Estate, Penicuik, Midlothian EH26 0QB, UK

7 ²School of Chemistry, University of Edinburgh, West Mains Road, Edinburgh EH9 3JJ,
8 UK

9
10 * contact author: email jnc@ceh.ac.uk telephone +44 (0)131 445 8533

11
12 **Abstract**

13 The reaction of ozone (O₃) with α -pinene has been studied as a function of temperature and
14 relative humidity and in the presence of wax surfaces that simulate a leaf surface. The
15 objective was to determine whether the presence of a wax surface, in which α -pinene could
16 dissolve and form a high surface concentration, would lead to enhanced reaction with O₃.

17 The reaction of O₃ itself with the empty stainless steel reactor and with aluminium and wax
18 surfaces demonstrated an apparent activation energy of around 30 kJ mol⁻¹ for all the
19 surfaces, similar to that observed in long-term field measurements of O₃ fluxes to
20 vegetation. However the absolute reaction rate was 14 times greater for aluminium foil and
21 saturated hydrocarbon wax surfaces than for stainless steel, and a further 5 times greater
22 for beeswax than hydrocarbon wax. There was no systematic dependence on either relative
23 or absolute humidity for these surface reactions over the range studied (20-100% RH).

24 Reaction of O₃ with α -pinene occurred at rates close to those predicted for the
25 homogeneous gas-phase reaction, and was similar for both the empty reactor and in the
26 presence of wax surfaces. The hypothesis of enhanced reaction at leaf surfaces caused by
27 enhanced surface concentrations of α -pinene was therefore rejected. Comparison of surface
28 decomposition reactions on different surfaces as reported in the literature with the results
29 obtained here demonstrate that the loss of ozone at the earth’s surface by decomposition to
30 molecular oxygen (i.e. without oxidative reaction with a substrate) can account for
31 measured ‘non-stomatal’ deposition velocities of a few mm s⁻¹. In order to quantify such
32 removal, the effective molecular surface area of the vegetation/soil canopy must be known.
33 Such knowledge, combined with the observed temperature dependence, provides necessary
34 input to global-scale models of O₃ removal from the troposphere at the earth’s surface.

1
2
3
4
5
6
7
8
9
10
11
12
13
14
15
16
17
18
19
20
21
22
23
24
25
26
27
28
29
30
31
32
33
34

Key words

Surface fluxes; dry deposition; biogenic VOCs; α -pinene; ozone destruction; leaf surface wax; epicuticular wax

Introduction

The removal of ozone (O_3) from the atmosphere by deposition at the earth's surface is an important process governing the budget of O_3 in the troposphere, and approximately balances the transport of O_3 downwards from the stratosphere into the troposphere (Lamarque, et al., 2005, Lelieveld and Dentener, 2000). Consequently, it is important to be able to measure and model the flux to the ground across a broad range of vegetation types and climatic conditions. Actual measurements of surface fluxes are difficult to make, as they are constrained by instrumental availability, and the need for appropriate micrometeorological conditions in which to make the measurements. Nevertheless, much progress has been made in understanding the contributory processes and sinks of O_3 , whether they be to soil, to water, to vegetation, or to the canopy space where biogenic emissions of O_3 -reactive compounds occur.

Interest in surface fluxes of O_3 has also been stimulated because of its reactivity towards plants, and consequent limitations on growth, or occurrence of visible damage symptoms. Several metrics for evaluating exposure, and relating exposure to effects, have been developed (Fuhrer, et al., 1997, Mauzerall and Wang, 2001), but there have been moves away from a simple exposure metric (measured as a product of O_3 concentration and time) to a metric based on the uptake of O_3 by plant leaves through stomata (Emberson, et al., 2000, Musselman and Massman, 1999). Measurements of the stomatal O_3 flux are inferred from measurements above plant canopies by assuming that the flux into leaves is proportional to the (measured) water vapour flux out of leaves when stomata are open, based simply on the relative rates of molecular diffusion of water vapour and O_3 to/from the sub-stomatal cavity (Altimir, et al., 2002, Zeller and Nikolov, 2000). The 'non-stomatal' flux is inferred by subtracting the calculated stomatal flux from the measured total flux. There is now a significant body of published literature for many plant types based on long-term measurements of O_3 fluxes. These measurements have consistently shown that surface fluxes can be divided into three components: stomatal uptake (relevant to effects), 'non-stomatal' uptake, and gas-phase reactions. Sometimes, the last two

1 processes are not distinguished; the former refers to assumed loss of O₃ on plant (or soil)
2 surfaces, and the latter refers to reactions of ozone with molecules such as nitric oxide
3 (NO) or biogenic volatile organic compounds (BVOCs) in the canopy space, or
4 immediately above the plant canopy, (e.g. Kurpius and Goldstein, 2003). However, the role
5 of biogenic VOCs may not be confined to gas-phase reactions; hydrocarbons dissolve in
6 plant surface waxes (Binnie, et al., 2002, Brown, et al., 1998), and may form high surface
7 concentrations, acting as a potential reactive sink in the leaf surface.

8
9 Leaf surfaces are coated with waxes, formed during leaf expansion and development. Most
10 of the components of plant waxes (at least for most temperate crop and forest species) are
11 saturated alkanes or oxygenated alkanes (Jetter, et al., 2006), i.e. without any obvious
12 reactive sites for O₃. The detailed mechanism of O₃ removal by the ‘non-stomatal’ route
13 (i.e. on leaf surfaces) is not known, although several researchers have demonstrated that
14 losses of O₃ other than through stomata can be the dominant sink for O₃ as an annual
15 budget. A combined measurement and modelling approach for a ponderosa pine forest in
16 southern California showed that 37% of the annual O₃ removal could be explained by in-
17 canopy gas-phase reactions, with 21.5% lost to surfaces and 41.5% to stomata (Kurpius
18 and Goldstein, 2003). Five years of measurement over a Norway spruce forest in Denmark
19 suggested that stomatal uptake only contributed 21% of the total O₃ flux (Mikkelsen, et al.,
20 2004); measurements during summer over a range of different vegetation types, when
21 stomatal uptake might be expected to be at a maximum, gave values between 14 and 69%
22 of the total (Cieslik, 2004); long-term measurements over moorland showed stomatal
23 uptake contributing only 30% of the total over 4 years (Fowler, et al., 2001). In these
24 examples no distinction was made between surface uptake and gas-phase reaction.
25 However, the overall removal rate can depend markedly on surface wetness (Altimir, et al.,
26 2006, Fuentes, et al., 1992, Grantz, et al., 1997, Grantz, et al., 1995, Lamaud, et al., 2002,
27 Pleijel, et al., 1995), suggesting a major role for surface removal. Both inhibition and
28 enhancement of O₃ fluxes to wet surfaces have been observed, depending on the plant
29 species under investigation.

30
31 This paper presents a study using simulated leaf surfaces to test the specific hypothesis that
32 surface reaction of O₃ with (dissolved) BVOCs can occur on leaf surfaces, thereby
33 enhancing the surface flux of O₃. The reaction rate of O₃ with α -pinene has been measured
34 in the absence and in the presence of wax-covered surfaces, simulating the epicuticular

1 surfaces of plant leaves. The reaction rate was studied over a range of ambient
2 temperatures and humidity.

4 **Methods**

5 *Reaction chamber*

6 All experiments took place in a Conviron CMP 3246 controlled environment exposure
7 cabinet, which enabled the overall control of temperature and relative humidity. The
8 reaction chamber itself, placed inside the cabinet, was made from stainless steel, with
9 internal dimensions of 0.5 m × 0.5 m × 1 m. Figure 1 shows a schematic of the
10 experimental system. Oxygen from an external cylinder was supplied to an electric
11 discharge O₃ generator (Dryden Aqua OZ500); for most experiments a constant O₃
12 production rate was used, which gave a concentration in the reaction chamber of around
13 130 ppb (parts in 10⁹ by volume). The O₃ source was diluted by charcoal-filtered air
14 pumped from within the cabinet; average flow rates of around 0.02 m³ min⁻¹ were recorded
15 using a dry-gas meter placed upstream of the pump. The exhaust air from the chamber was
16 vented to the outside of the building through a mirror dewpoint meter (Michell Instruments
17 Series 3000). Temperatures inside the chamber were recorded using a chromel/alumel K-
18 type thermocouple.

19
20 The inlet O₃ sampling line (0.125" o.d. stainless steel) was sealed to the interior of the
21 chamber so as to sample from the inlet air as it entered the chamber, thereby ensuring that
22 sampling was undertaken at the chamber internal pressure, rather than the slightly higher
23 pressure of the inlet tube itself. The outlet air stream was sampled immediately
24 downstream of the reaction chamber. The inlet and outlet air streams were alternately
25 sampled over five minute periods, using a 3-way stainless steel solenoid valve controlled
26 by a Campbell Scientific 21X micrologger. The first minute's data after switching the
27 valve were not used for data analysis. O₃ concentrations in the inlet and outlet air were
28 measured using a Thermo Environmental Instruments 49C O₃ analyser (dual channel, UV
29 absorption, nominal precision 1 ppb). Mixing within the chamber was achieved using a
30 stainless steel fan mounted on one wall; the efficiency of mixing was measured by using an
31 O₃-reactive surface sink to assess the maximum surface flux achievable (see later).

32 33 *Methods for generating controlled α-pinene concentrations*

1 α -Pinene was introduced into the chamber using a diffusion source. After several trials of
2 different methods, a reliable source with the appropriate release rate to provide an air
3 concentration of around $100 \mu\text{g m}^{-3}$ was devised by placing 0.5 ml pure α -pinene (Sigma-
4 Aldrich, as received) in a 2 ml glass sample vial sealed with a polyethylene plug
5 (Chromacol) that was slightly permeable to the vapour. The vial was maintained at the
6 constant temperature of the cabinet inside a glass bottle through which a charcoal-filtered
7 air flow of around $0.002 \text{ m}^3 \text{ min}^{-1}$ was maintained, leading into the reaction chamber.
8 Measurements made over a period of up to 24 days and over a range of temperatures (5 to
9 $35 \text{ }^\circ\text{C}$) showed that the rate of mass loss was approximately linear for a given vial, at ca. 3
10 mg d^{-1} . The rate varied from vial to vial and was not predictably related to temperature, so
11 the mass of each sample vial was measured at the beginning and end of each experiment,
12 and the average α -pinene concentration was calculated based on the change in mass and
13 the measured overall air flow rate through the chamber.

14

15 *Methods for producing wax surfaces*

16 To prepare a model leaf surface, a stainless steel plate ($0.31 \text{ m} \times 0.71 \text{ m}$) was covered with
17 a pre-weighed sheet of aluminium foil as a substrate for wax deposition. For the
18 experiments a target wax coverage of 1 mg cm^{-2} was used, equivalent to 2.20 g for the area
19 of the steel plate. This mass of wax was dissolved in 25 ml of dichloromethane at $40 \text{ }^\circ\text{C}$
20 then decanted in 3 aliquots into a small glass bottle attached to a spray nebulizer (Badger
21 Airbrush) driven by a compressed gas propellant. The contents of the bottle were then
22 evenly sprayed onto the foil-covered plate in a fume cupboard. Rapid evaporation of the
23 dichloromethane produced an even coating of wax on the Al foil. The process was repeated
24 with the remaining two aliquots to ensure that the plate was adequately covered. The actual
25 mass of wax on the foil surface was determined by weighing the wax-coated foil at the end
26 of each experiment.

27

28 *Data analysis techniques*

29 The removal of O_3 within the empty reaction chamber was calculated from the difference
30 in O_3 concentrations between the inlet and outlet ($\Delta[\text{O}_3]$), the air flow rate (F), the internal
31 surface wall area (A) and the well-mixed (outlet) concentration $[\text{O}_3]$, to give a removal
32 'resistance' (R_w) having units of s m^{-1} :

$$R_w = \frac{[O_3] \cdot A}{\Delta[O_3] \cdot F} \quad (1)$$

R_w was measured as a function of temperature between 10 and 35 °C. This overall resistance comprises a turbulent transfer resistance to the surface (R_t) and a surface resistance (R_s), acting in series.

The mass flux of O_3 to the stainless steel walls of the chamber is given by:

$$[O_3]/R_w \text{ g m}^{-2} \text{ s}^{-1}$$

where concentration is expressed in g m^{-3} ,

and the loss rate to the walls is then:

$$A \cdot [O_3]/R_w = \Delta[O_3] \cdot F \text{ g s}^{-1}.$$

11

In order to estimate the transfer resistance (R_t), which was assumed to be invariant for fixed air flow rates and fan mixing speed, a sheet of plastic-backed absorbent paper, thoroughly wetted with potassium iodide solution (which reacts rapidly with O_3) was introduced into the base of the chamber. The overall loss of O_3 measured as $\Delta[O_3] \cdot F$ was then equated to the loss to the steel walls $(A - A_{\text{abs}}) \cdot [O_3]/R_w$ plus the loss to the absorbent surface $A_{\text{abs}} \cdot [O_3]/R_{\text{abs}}$, where A_{abs} is the area of the absorbent paper. The value of $R_{\text{abs}} = R_t + (R_s)_{\text{abs}}$ can thus be obtained, and is taken to be equivalent to R_t , on the assumption that $(R_s)_{\text{abs}}$ is effectively zero for the reactive absorbent surface. Four replicate experiments over a period of a month gave a value for $R_{\text{abs}} \sim R_t$ of $206 (\pm 25) \text{ s m}^{-1}$. This is negligible relative to typical values of R_w of around $3 \times 10^4 \text{ s m}^{-1}$ (see below), and indicates good mixing within the reaction chamber.

23

In order to test the uptake of O_3 by different surfaces, the steel plate covered in a sheet of aluminium foil (with and without a wax coating) was introduced, and a similar set of calculations undertaken using the values of R_w and R_t to measure R_s for the different surfaces over a range of temperatures.

28

A similar calculation was done in the presence of α -pinene, where an additional O_3 loss term was included:

31

$$\Delta[O_3] \cdot F = (A - A_s) \cdot [O_3]/R_w + A_s \cdot [O_3]/R_s + k \cdot V \cdot [O_3] \cdot [\alpha\text{-pinene}] \quad (2)$$

1
2 where V is the volume of the reaction chamber (0.25 m^3).

3
4 In this case the reaction rate coefficient ($k, \text{m}^3 \text{g}^{-1} \text{s}^{-1}$) includes both the homogeneous gas-
5 phase reactions of O_3 with α -pinene, and any reactions occurring at the walls or other
6 surfaces in the chamber. Only the inlet concentration of α -pinene is known (from the
7 diffusion source), so the effective well-mixed concentration of α -pinene to be used in
8 Equation 2 was calculated by assuming that the initial reaction with O_3 had unit molar
9 stoichiometry. In a typical experiment, α -pinene was introduced to the chamber and
10 allowed to equilibrate with the wax-coated Al foil (2-3 h) before introduction of O_3 . After a
11 new equilibrium had been established, the reaction rate was measured, then the α -pinene
12 source was turned off, and a new equilibrium was established for the box containing the
13 wax plate. The reaction rate with α -pinene was taken as the simple difference between the
14 two reaction rates, with and without α -pinene present. In some experiments the α -pinene
15 source was repeatedly attached and removed; no significant hysteresis was observed.

16 17 **Results**

18 *Empty box (reaction of O_3 with stainless steel)*

19 Over 50 experiments were conducted over a period of 14 months, at temperatures between
20 8 and 33 °C and dew points between 6 and 19 °C. There was a strong dependence of the
21 surface resistance (R_s) on temperature (Figure 2), and although there was some variation
22 between experiments, this was not related to water vapour concentration, whether
23 expressed as absolute or relative humidity. The dependence can be expressed in an
24 Arrhenius form:

$$25 \ln(R_s) = 31.3 (\pm 4.1) \times 10^3/RT + 0.2 (\pm 1.7) \quad (3)$$

26
27
28 where the error terms are the standard errors of the fitted parameters. The Pearson
29 correlation coefficient (r^2) was 0.52. This implies a reaction with an activation energy of
30 31 kJ mol^{-1} . In all, 22 experiments were conducted at a temperature of $23.5 (\pm 0.3) \text{ }^\circ\text{C}$, with
31 an average absolute value of R_s of $4.4 (\pm 0.8) \times 10^5 \text{ s m}^{-1}$; the predicted value from
32 Equation 3 is $4.0 \times 10^5 \text{ s m}^{-1}$.

1 There was some evidence of a general increase in variability over time. The data from the
2 24 experiments in April 2005 were best fitted by:

$$3 \ln(R_s) = 40.1 (\pm 3.8) \times 10^3/RT - 3.28 (\pm 1.55) \quad (4)$$

4 with an r^2 of 0.84,

5 while the data from the 31 experiments in June 2006 were best fitted by:

$$6 \ln(R_s) = 15.2 (\pm 5.9) \times 10^3/RT + 6.6 (\pm 2.4) \quad (5)$$

7 but this relationship, although statistical significant, had an r^2 of only 0.19.

8

9 The respective predicted and measured values at 23.5 °C were $4.3 \times 10^5 \text{ s m}^{-1}$ (Eqn.4)
10 (measured $4.5 (\pm 1.0) \times 10^5$) and $3.5 \times 10^5 \text{ s m}^{-1}$ (Eqn.5) (measured $4.4 (\pm 0.8) \times 10^5$),
11 respectively.

12

13 In the following calculations for estimating fluxes to other surfaces in the reaction
14 chamber, the rate of loss to the steel walls (which must be subtracted from the overall
15 ozone loss to obtain the rate of loss to the other surface) was calculated using either
16 Equation 4 or Equation 5, depending on the date of the experiments.

17

18 *Flux to aluminium foil*

19 Aluminium foil was used as a substrate for building the artificial leaf surfaces, so the flux
20 and reaction of O₃ with the bare surface was measured in a series of 30 experiments over a
21 range of temperatures. The results are shown in Figure 2. The typical uncertainty
22 (combined error from the calculation) for each value is 15%. As for the steel walls, the
23 surface flux increased with temperature with an apparent activation energy of $25 (\pm 8) \text{ kJ}$
24 mol^{-1} . The reaction rate with Al foil was significantly greater than with stainless steel; the
25 predicted R_s at 23.5 °C was $2.8 \times 10^4 \text{ s m}^{-1}$ compared with $4.0 \times 10^5 \text{ s m}^{-1}$ for steel.

26

27 *Flux to paraffin wax*

28 The first artificial leaf surface to be constructed was made from paraffin wax (melting
29 point 49-52 °C, Fisher Chemicals, Loughborough, UK, used as received) as described
30 above, with an average wax loading of 0.4 mg cm^{-2} on the Al foil. The results are shown in
31 Figure 2, again with an apparent activation energy, of $23 (\pm 19) \text{ kJ mol}^{-1}$, although the
32 uncertainty on this is much larger than for the uncoated foil, partly because of the smaller

1 number of experiments (9). The absolute values of R_s were not significantly different from
2 those for the substrate Al foil. No effect of differences in surface coverage was observed.

3 4 *Flux to beeswax*

5 Beeswax was chosen as a potentially ozone-reactive wax, as it contains unsaturated long-
6 chain hydrocarbons. The surface flux to beeswax (refined, yellow, ACROS Organics, Geel,
7 Belgium, used as received) was significantly faster than to paraffin wax, even though the
8 coverage achieved in the experiments was variable, and on average only 0.1 mg cm^{-2} . The
9 apparent activation energy from 10 experiments at a range of temperatures was $16 (\pm 6) \text{ kJ}$
10 mol^{-1} , and there was no obvious dependence on the wax coverage achieved. However, the
11 overall rate of reaction was almost 5 times greater than to paraffin wax or Al foil, with an
12 estimated R_s at $23.5 \text{ }^\circ\text{C}$ of $6.0 \times 10^3 \text{ s m}^{-1}$. This surface resistance is still 30 times greater
13 than the estimated gas-phase transfer resistance (R_t) measured for the ‘perfect’ sink
14 surface, so reaction rates at the surface were controlled by the surface itself rather than by
15 rates of transfer from the gas-phase.

16 17 *Reactions with α -pinene*

18 An initial set of experiments investigated the reactions of O_3 with α -pinene in the empty
19 steel box. The loss of O_3 in the box was measured with and without the addition of a
20 known mass flow of α -pinene, and the difference in O_3 loss is attributed to the sum of the
21 gas-phase reaction of O_3 with α -pinene and any reactions which may have occurred on the
22 wall surfaces. A set of 7 experiments, all at $23.5 \text{ }^\circ\text{C}$, gave an effective rate coefficient for
23 the reaction of $1.4 (\pm 0.4) \times 10^{-16} \text{ cm}^3 \text{ molec}^{-1} \text{ s}^{-1}$, where the uncertainty is the standard
24 deviation ($n = 7$). Introduction of the Al foil made little difference to the effective rate
25 coefficient, for 5 experiments at $3.6 \text{ }^\circ\text{C}$ and 2 experiments at $33.5 \text{ }^\circ\text{C}$ (Figure 3), where the
26 values of k were $8.6 (\pm 2.1) \times 10^{-17} \text{ cm}^3 \text{ molec}^{-1} \text{ s}^{-1}$ and $2.0 (\pm 0.2) \times 10^{-16} \text{ cm}^3 \text{ molec}^{-1} \text{ s}^{-1}$,
27 respectively.

28
29 The original hypothesis – that O_3 and α -pinene react on leaf surfaces in addition to the gas-
30 phase, because of the presence of epicuticular waxes – was then tested by reacting α -
31 pinene with O_3 with a wax-coated foil surface in the chamber. In these experiments, the α -
32 pinene was introduced first and allowed to equilibrate with the wax surface before the O_3
33 was introduced, and the steady-state removal rate measured. The α -pinene source was then

1 removed, and the subsequent reaction of O₃ with the surfaces in the box was measured,
2 again after several hours equilibration, by which time any α-pinene that had been adsorbed
3 on the wax surface would have desorbed and left the reactor. The results of 2 experiments
4 at each of 3 temperatures (3.6, 23.5 and 33.7 °C) are shown in Figure 3. The reaction rate
5 between O₃ and α-pinene in the presence of a wax surface is not significantly different
6 from that with the empty box, i.e. the hypothesis that the solution /adsorption of α-pinene
7 in the surface wax leads to enhanced removal of O₃ by reaction with adsorbed α-pinene,
8 has to be rejected. Similar results were found in 6 experiments with beeswax (Figure 3).

10 Discussion

11 Interest in the rate of reaction of O₃ with surfaces has led to experimental studies by a
12 range of different researchers: losses of O₃ to dust particles in the atmosphere, such as soot
13 (Kamm, et al., 1999), or mineral dust (Hanisch and Crowley, 2003, Sullivan, et al., 2004),
14 have been studied in a variety of experimental systems. As part of these studies, loss rates
15 to ‘inert’ surfaces have also been measured. Although there have been no controlled
16 laboratory measurements of loss rates to plant leaf surfaces prior to this study, interest in
17 O₃ losses and reactions in indoor environments has led to several studies of O₃ reaction on
18 the surfaces of building materials and furnishings (Grøntoft and Raychaudhuri, 2004,
19 Nicolas, et al., 2007), particularly in aircraft (Coleman, et al., 2008). The deliberate
20 removal of O₃ from air has received considerable interest in terms of suitable catalysts
21 (Dhandapani and Oyama, 1997) or absorbents such as activated charcoal . Each discipline
22 has used slightly different methods of expressing their results: the rate of O₃ loss may be
23 expressed in terms of the reaction probability (γ), or as a deposition velocity (v_d), with
24 appropriate correction for the rate of transfer of O₃ molecules to the reacting surface. These
25 different measures may be related to the surface resistance (R_s) used in this study by the
26 following:

27
28 $R_s = 1/v_d$, where v_d is corrected for turbulent transfer to the surface

29
30 $R_s = 4/(\gamma \cdot \langle v \rangle)$, where <v> is the mean Boltzmann collision velocity for O₃ molecules at a
31 surface, dependent upon (temperature)^{1/2} and molecular mass, and equivalent to 360 m s⁻¹
32 at 293 K.

1 In some experiments, results are expressed in terms of a first-order rate coefficient for wall
2 reactions (k) that can be related to R_s by:

3
4 $R_s = A/(k.V)$, where A and V are the internal surface area and volume of the reactor,
5 respectively.

6
7 Given these conversion equations, the results from this experiment can be set in the context
8 of a wide range of similar data relating to reaction and/or decomposition of O_3 on solid
9 surfaces. A summary of O_3 fluxes to a range of relevant surfaces is shown in Table 1,
10 converted into the same units of surface resistance (R_s) as given above. Many of these refer
11 to instantaneous reaction rates, which change with time during an experiment, rather than
12 those that would apply at equilibrium under steady-state conditions, as in our experiments.

13
14 There have been few systematic studies of the temperature-dependence of this reaction,
15 although an apparent activation energy for reaction with dry soot aerosol during the ‘slow
16 reaction’ phase of 46 kJ mol^{-1} has been measured (Kamm, et al., 1999). Although this is
17 similar to the values observed in this study (Figure 2), the reaction with soot is
18 undoubtedly more complex than with the ‘inert’ surfaces used here (steel, Al foil and wax),
19 but may reflect the underlying energy dependence of the heterogeneous decomposition of
20 O_3 to O_2 which is suggested as the rate-determining step. In many of the studies with
21 mineral dust aerosols, surfaces show a very rapid uptake of O_3 followed by a slower rate of
22 O_3 loss, and gradual deactivation of the surface, accompanied by evolution of molecular O_2
23 (Karagulian and Rossi, 2006). In our study, the initial reaction rate was not recorded, only
24 the steady-state condition after several hours’ exposure.

25
26 The effects of humidity have been studied in some experiments, although many of the
27 measurements have been made in totally dry air, in very different conditions from those
28 that would obtain in the real troposphere. Where O_3 loss rates have been measured
29 explicitly as a function of humidity, initial rapid reaction rates in dry air were greatly
30 reduced as humidity increased, leading to a lower ‘plateau’ at $RH > 30\%$ (Mogili, et al.,
31 2006). This behaviour is interpreted as competition between water vapour and O_3
32 molecules for active sites on the aerosol surface, and the eventual accumulation of several
33 monolayers of water on the surface at $RH > 30\%$. However, for ‘aged’ or reactive surfaces,
34 the surface resistance tends to decrease as humidity increases (Table 1), but in some

1 experiments no dependence on humidity was observed (Sullivan, et al., 2004). These
2 observations confirm the lack of humidity dependence noted in our study, where RH varied
3 only between 20 and 100%, and ‘aged’ surfaces were used. In controlled experiments with
4 artificial mineral substrates, surface wetness or layers of water on the surface would not
5 lead to the dissolution or leaching of O₃-reactive materials, and the reaction of O₃ at the
6 surface may appear similar to reaction with pure water, albeit modified by being
7 constrained to a surface layer (Grøntoft, et al., 2004). However, for potentially reactive
8 surfaces such as wood or leaves, surface wetness may also lead to leaching or dissolution
9 of materials from the surface, and these (rather than simple decomposition of O₃) may
10 determine the actual surface resistance and surface flux of O₃ to field-grown plants.

11

12 In general, the initial reaction rates with surfaces are reported to be higher at smaller
13 concentrations of O₃, interpreted as a feature of surface saturation of reactive sites, albeit
14 partially reversible by removing O₃. The initial rates reported in Table 1 refer to a system
15 which is not in steady state, in contrast to the conditions in our experiments, where the
16 observed removal rates are under thermodynamic rather than kinetic control. In one study
17 (Mogili, et al., 2006), the reaction rate at high humidity appeared to be zero-order in O₃.
18 The order of the reaction was not studied in our experiments, because the inlet O₃
19 concentration was approximately constant.

20

21 The following conclusions may be drawn from Table 1: ‘inert’ surfaces such as glass,
22 PTFE or stainless steel have high surface resistances, while Al has a lower surface
23 resistance, possibly because metallic Al exposed to the atmosphere is covered in a thin
24 oxide (Al₂O₃) layer, and therefore behaves in a similar way to Al₂O₃ aerosol particles,
25 which have been the subject of several experimental studies (Mogili, et al., 2006, Sullivan,
26 et al., 2004, Usher, et al., 2003). Non-reactive (alkane) wax layers might be expected to
27 show similar reactivity to paints or plastics, and this is indeed observed, while untreated
28 wood surfaces are more reactive, and approach the reactivity of living plant material.

29

30 The results presented above for reactions in the absence of α -pinene show that the ‘steady-
31 state’ loss of O₃ on ‘inert’ surfaces is temperature-dependent, with a common apparent
32 activation energy of around 30 kJ mol⁻¹. This suggests that O₃ is lost through
33 heterogeneous decomposition at the surface. The absolute reaction rate depends on other
34 properties of the surface; stainless steel was least reactive of all the surfaces studied,

1 approximately 14 times less reactive (as measured by the surface resistance) than
2 aluminium foil or paraffin wax. This is consistent with earlier data (see Table 1), where R_s
3 for stainless steel was 6.5 times greater than for aluminium when measured in the same
4 apparatus (Cano-Ruiz, et al., 1993). The additional reactivity of aluminium (coated in a
5 surface layer of Al_2O_3) may relate to the availability of surface reaction sites for O_3
6 adsorption and reaction, as noted by authors who have investigated O_3 uptake and reaction
7 on Al_2O_3 aerosols (Mogili, et al., 2006, Sullivan, et al., 2004, Usher, et al., 2003).

8
9 The similar reactivity of the paraffin wax surface may reflect the full saturation of the wax
10 molecules, in contrast to polyethylene, which appears to be more reactive (lower R_s) than
11 aluminium when compared in the same experiment (Table 1). Although chemically similar
12 to a saturated wax surface, the polymer may still contain a significant number of reactive
13 sites for O_3 . The 5-times greater reactivity of beeswax in our experiments can be ascribed
14 to the presence of unsaturated molecules in the beeswax, and/or may be because of a
15 rougher surface structure. An experiment using C_8 -alkene and C_8 -alkane coatings on silica
16 particles showed a 2-fold larger initial reaction rate for an alkene-coated surface than an
17 alkane-coated surface (Usher, et al., 2003). The absolute resistances for these reactions in
18 Table 1 refer to the initial reaction rates, which decreased markedly with exposure time, so
19 cannot be compared directly with the values obtained in our experiments.

20
21 In studies of powders and building materials, the accessible surface area (as opposed to the
22 geometric surface area) is explicitly measured as an important factor in normalising the
23 chemical reaction rate. For vegetation, this is explicitly taken into account in many dry
24 deposition models, even though deposition velocities (and surface resistances) measured
25 above a vegetation canopy are usually expressed in terms of the geometric land area below
26 the measurement point. This has to be multiplied by the (two-sided) leaf area index (LAI)
27 as a measure of the effective surface area accessible for O_3 destruction. Moreover, the fine-
28 scale structure of leaf surfaces, which may be covered in trichomes or semi-crystalline
29 epicuticular waxes, should also be considered. For example, a Scots pine needle surface is
30 covered in C_{29} -alkanol wax tubes, typically $1.5 \mu m$ long and $150 nm$ in diameter, at a
31 density of $10 \text{ tubes } \mu m^{-2}$ (Crossley and Fowler, 1986), leading to an increase in surface
32 area by a factor of 7 relative to a smooth wax surface, even without consideration of the
33 effective area at the molecular scale. The effective area available for O_3 destruction of a
34 plant canopy with a (two-sided) LAI of 5, typical of a Scots pine forest (Bealde, et al.,

1 1982), may therefore be over 30 times the ground area, and it should therefore not be
2 surprising that the surface resistance for O₃ loss to vegetation is as low as several hundred s
3 m⁻¹ when the surface resistance for an ‘inert’ smooth wax surface is 3 × 10⁴ s m⁻¹, as
4 measured in this study. No chemical reaction of O₃ with a reactive substance at the surface
5 is required – the heterogeneous decomposition of O₃ to molecular O₂ would be expected to
6 occur at rates similar to this on all surfaces exposed to a humid atmosphere.

7

8 **Conclusions**

9 Ozone is generally regarded as having a very low rate of reaction or decomposition at
10 ‘inert’ surfaces, as shown for stainless steel in the experimental results reported here. For
11 more polar surfaces, because of surface oxide groups and/or the presence of thin layers of
12 water molecules (as would be expected for polar surfaces in most tropospheric situations),
13 the decomposition of O₃ is enhanced relative to ‘inert’ surfaces, even on surfaces that are
14 well ‘aged’ and where specific surface reaction sites have been reacted or blocked. The
15 apparent activation energy for this reaction is around 30 kJ mol⁻¹, leading to an increase in
16 the removal rate at the surface with ambient temperatures by a factor of 2 between 9 and
17 25 °C. The absolute reaction rate appears to depend on the effective surface area at a
18 microscopic scale. Although this is explicitly recognised when dealing with dusts or
19 aerosols, it may not be appreciated just how great the effective surface of a plant canopy
20 may be for O₃ removal. A simple calculation for one type of forest indicates that this area
21 may be over 30 times the ground area. Consequently, a surface resistance of 2 × 10⁴ s m⁻¹
22 for a smooth ‘inert’ surface measured in the laboratory at >50% relative humidity could
23 correspond to a canopy surface resistance of a few hundred s m⁻¹ (equivalent to a
24 deposition velocity of a few mm s⁻¹) if the only process removing O₃ were decomposition
25 at the complex surface of the foliage. In the presence of light, with the potential for
26 photolytic processes to contribute to O₃ reactions, and in the presence of a range of
27 material present on the canopy surface (from prior deposition, from biota on the leaf
28 surface, or from leaching from inside the leaf), the potential removal rate at a canopy could
29 be very much greater. If such processes are to be incorporated explicitly into models of the
30 removal of O₃ at the earth’s surface, for example for use in global climate and chemistry
31 modelling, then the above measurements give an indication of the likely temperature
32 response, and indicate the need for the measurement or estimation of the actual canopy
33 surface responsible for the removal of O₃ by heterogeneous decomposition.

1
2
3
4
5
6
7
8
9
10
11
12
13
14
15
16
17
18
19
20
21
22
23
24
25
26
27
28
29
30
31
32
33
34
35
36
37
38
39
40
41
42

References

Altimir N., Kolari P., Tuovinen J.P., Vesala T., Back J., Suni T., Kulmala M., Hari P., 2006. Foliage surface ozone deposition: a role for surface moisture? *Biogeosciences* **3**, 209-228

Altimir N., Vesala T., Keronen P., Kulmala M., Hari P., 2002. Methodology for direct field measurements of ozone flux to foliage with shoot chambers. *Atmospheric Environment* **36**, 19-29

Bealde C.L., Talbot H., Jarvis P.G., 1982. Canopy Structure and Leaf Area Index in a Mature Scots Pine Forest. *Forestry* **55**, 105-123

Binnie J., Cape J.N., Mackie N., Leith I.D., 2002. Exchange of organic solvents between the atmosphere and grass - the use of open top chambers. *Science of the Total Environment* **285**, 53-67

Brown R.H.A., Cape J.N., Farmer J.G., 1998. Partitioning of chlorinated solvents between pine needles and air. *Chemosphere* **36**, 1799-1810

Cano-Ruiz J.A., Kong D., Balas R.B., Nazaroff W.W., 1993. Removal of reactive gases at indoor surfaces - combining mass transport and surface kinetics. *Atmospheric Environment Part a-General Topics* **27**, 2039-2050

Cieslik S.A., 2004. Ozone uptake by various surface types: a comparison between dose and exposure. *Atmospheric Environment* **38**, 2409-2420

Coleman B.K., Destailhats H., Hodgson A.T., Nazaroff W.W., 2008. Ozone consumption and volatile byproduct formation from surface reactions with aircraft cabin materials and clothing fabrics. *Atmospheric Environment* **42**, 642-654

Crossley A., Fowler D., 1986. The weathering of Scots pine epicuticular wax in polluted and clean air. *New Phytologist* **103**, 207-218

Dhandapani B., Oyama S.T., 1997. Gas phase ozone decomposition catalysts. *Applied Catalysis B-Environmental* **11**, 129-166

Emberson L.D., Ashmore M.R., Cambridge H.M., Simpson D., Tuovinen J.P., 2000. Modelling stomatal ozone flux across Europe. *Environmental Pollution* **109**, 403-413

Fowler D., Flechard C., Cape J.N., Storeton-West R.L., Coyle M., 2001. Measurements of ozone deposition to vegetation quantifying the flux, the stomatal and non-stomatal components. *Water Air and Soil Pollution* **130**, 63-74

Fuentes J.D., Gillespie T.J., Denhartog G., Neumann H.H., 1992. Ozone Deposition onto a Deciduous Forest During Dry and Wet Conditions. *Agricultural and Forest Meteorology* **62**, 1-18

Fuhrer J., Skarby L., Ashmore M.R., 1997. Critical levels for ozone effects on vegetation in Europe. *Environmental Pollution* **97**, 91-106

Grantz D.A., Zhang X.J., Massman W.J., Delany A., Pederson J.R., 1997. Ozone deposition to a cotton (*Gossypium hirsutum* L) field: stomatal and surface wetness

- 1 effects during the California Ozone Deposition Experiment. *Agricultural and*
2 *Forest Meteorology* **85**, 19-31
- 3 Grantz D.A., Zhang X.J., Massman W.J., DenHartog G., Neumann H.H., Pederson J.R.,
4 1995. Effects of stomatal conductance and surface wetness on ozone deposition in
5 field-grown grape. *Atmospheric Environment* **29**, 3189-3198
- 6 Grøntoft T., Henriksen J.F., Seip H.M., 2004. The humidity dependence of ozone
7 deposition onto a variety of building surfaces. *Atmospheric Environment* **38**, 59-68
- 8 Grøntoft T., Raychaudhuri M.R., 2004. Compilation of tables of surface deposition
9 velocities for O₃, NO₂ and SO₂ to a range of indoor surfaces. *Atmospheric*
10 *Environment* **38**, 533-544
- 11 Grosjean D., 1985. Wall loss of gaseous pollutants in outdoor Teflon chambers.
12 *Environmental Science & Technology* **19**, 1059-1065
- 13 Hanisch F., Crowley J.N., 2003. Ozone decomposition on Saharan dust: an experimental
14 investigation. *Atmospheric Chemistry and Physics* **3**, 119-130
- 15 IUPAC, 2007. Data sheet Ox_VOC8 (17/12/07), [http://www.iupac-](http://www.iupac-kinetic.ch.cam.ac.uk/datasheets/gas/Ox_VOC8_O3_apinene.pdf)
16 [kinetic.ch.cam.ac.uk/datasheets/gas/Ox_VOC8_O3_apinene.pdf](http://www.iupac-kinetic.ch.cam.ac.uk/datasheets/gas/Ox_VOC8_O3_apinene.pdf), (ed.),
- 17 Jetter R., Kunst L., Samuels A.L., 2006. Composition of plant cuticular waxes, in: Riederer
18 M., Muller C. (ed.), *Biology of the Plant Cuticle*, Wiley-Blackwell, Oxford,
- 19 Kamm S., Mohler O., Naumann K.H., Saathoff H., Schurath U., 1999. The heterogeneous
20 reaction of ozone with soot aerosol. *Atmospheric Environment* **33**, 4651-4661
- 21 Karagulian F., Rossi M.J., 2006. The heterogeneous decomposition of ozone on
22 atmospheric mineral dust surrogates at ambient temperature. *International Journal*
23 *of Chemical Kinetics* **38**, 407-419
- 24 Kerstiens G., Lenzian K.J., 1989. Interactions between ozone and plant cuticles.1. Ozone
25 deposition and permeability. *New Phytologist* **112**, 13-19
- 26 Kurpius M.R., Goldstein A.H., 2003. Gas-phase chemistry dominates O₃ loss to a forest,
27 implying a source of aerosols and hydroxyl radicals to the atmosphere. *Geophysical*
28 *Research Letters* **30**
- 29 Lamarque J.F., Hess P., Emmons L., Buja L., Washington W., Granier C., 2005.
30 Tropospheric ozone evolution between 1890 and 1990. *Journal of Geophysical*
31 *Research-Atmospheres* **110**
- 32 Lamaud E., Carrara A., Brunet Y., Lopez A., Druilhet A., 2002. Ozone fluxes above and
33 within a pine forest canopy in dry and wet conditions. *Atmospheric Environment*
34 **36**, 77-88
- 35 Lelieveld J., Dentener F.J., 2000. What controls tropospheric ozone? *Journal of*
36 *Geophysical Research-Atmospheres* **105**, 3531-3551
- 37 Mauzerall D.L., Wang X., 2001. Protecting agricultural crops from the effects of
38 tropospheric ozone exposure: reconciling science and standard setting in the United
39 States, Europe and Asia. *Annual Review of Energy and the Environment* **26**, 237-
40 268
- 41 Mikkelsen T.N., Ro-Poulsen H., Hovmand M.F., Jensen N.O., Pilegaard K., Egelov A.H.,
42 2004. Five-year measurements of ozone fluxes to a Danish Norway spruce canopy.
43 *Atmospheric Environment* **38**, 2361-2371

- 1 Mogili P.K., Kleiber P.D., Young M.A., Grassian V.H., 2006. Heterogeneous uptake of
2 ozone on reactive components of mineral dust aerosol: An environmental aerosol
3 reaction chamber study. *Journal of Physical Chemistry A* **110**, 13799-13807
- 4 Musselman R.C., Massman W.J., 1999. Ozone flux to vegetation and its relationship to
5 plant response and ambient air quality standards. *Atmospheric Environment* **33**, 65-
6 73
- 7 Nicolas M., Ramalho O., Maupetit F., 2007. Reactions between ozone and building
8 products: Impact on primary and secondary emissions. *Atmospheric Environment*
9 **41**, 3129-3138
- 10 Pleijel H., Karlsson G.P., Danielsson H., Sellden G., 1995. Surface wetness enhances
11 ozone deposition to a pasture canopy. *Atmospheric Environment* **29**, 3391-3393
- 12 Sullivan R.C., Thornberry T., Abbatt J.P.D., 2004. Ozone decomposition kinetics on
13 alumina: effects of ozone partial pressure, relative humidity and repeated oxidation
14 cycles. *Atmospheric Chemistry and Physics* **4**, 1301-1310
- 15 Tillmann R., Mentel T.F., Kiendler-Scharr A., Brauers T., Saathof H., 2007. Temperatur
16 dependent rate coefficients of the α -pinene + ozone reaction. *Geophysical Research*
17 *Abstracts* **9**, 09179
- 18 Usher C.R., Michel A.E., Stec D., Grassian V.H., 2003. Laboratory studies of ozone
19 uptake on processed mineral dust. *Atmospheric Environment* **37**, 5337-5347
- 20 Zeller K.F., Nikolov N.T., 2000. Quantifying simultaneous fluxes of ozone, carbon dioxide
21 and water vapor above a subalpine forest ecosystem. *Environmental Pollution* **107**,
22 1-20
- 23

Table 1. Summary of relevant surface ozone loss data for temperatures 10-30 °C and 1 atm total pressure (unless otherwise indicated), expressed as surface resistance (R_s) ($s\ m^{-1}$)

Surface	ppb O ₃		RH (%)		R_s ($s\ m^{-1}$ /1000)	comment	Reference
	where given	where given	where given	where given			
clean glass					2	calc. from Simmons and Colbeck, 1990	(Cano-Ruiz, et al., 1993)
plate glass					202	Aged; calc. from Sabersky et al., 1975	(Cano-Ruiz, et al., 1993)
glass	105	48			1429		(Nicolas, et al., 2007)
glass	160	52			625		(Nicolas, et al., 2007)
PTFE film	340-1550	dry air			654		(Grosjean, 1985)
FEP Teflon					20	calc. from Simmons and Colbeck, 1990	(Cano-Ruiz, et al., 1993)
teflon					556	calc. from Altshuller and Wartburg, 1961	(Cano-Ruiz, et al., 1993)
stainless steel					12	Aged; calc. from Mueller et al., 1973	(Cano-Ruiz, et al., 1993)
stainless steel					2778	calc. from Tkalich et al., 1984; low press.	(Cano-Ruiz, et al., 1993)
stainless steel					556	calc. from Altshuller and Wartburg, 1961	(Cano-Ruiz, et al., 1993)
stainless steel	140	50-90			440		this study
aluminium					202	Aged; calc. from Sabersky et al., 1975	(Cano-Ruiz, et al., 1993)
aluminium		5			227	calc. from Mueller et al., 1973	(Cano-Ruiz, et al., 1993)
aluminium		40-50			85	Aged; calc. from Mueller et al., 1973	(Cano-Ruiz, et al., 1993)
aluminium		87			5	calc. from Mueller et al., 1973	(Cano-Ruiz, et al., 1993)
aluminium		32			144	calc. from Cox & Penkett, 1972	(Cano-Ruiz, et al., 1993)
aluminium		83			48	calc. from Cox & Penkett, 1972	(Cano-Ruiz, et al., 1993)
aluminium					85	calc. from Altshuller and Wartburg, 1961	(Cano-Ruiz, et al., 1993)
aluminium	150	dry air			15	assumes V/A=1	(Kamm, et al., 1999)
aluminium foil	130	50-90			28		this study
Al ₂ O ₃					1	initial uptake rate; pressure 10-70 Pa	(Sullivan, et al., 2004)

Saharan dust	>10 ⁸	dry N ₂	6	total pressure < 0.13 Pa	(Hanisch and Crowley, 2003)
C8-alkene on SiO ₂	10 ⁸	dry	0.2	initial uptake rate; total pressure 0.009 Pa	(Usher, et al., 2003)
C8-alkane on SiO ₂	10 ⁸	dry	0.4	initial uptake rate; total pressure 0.009 Pa	(Usher, et al., 2003)
polyethylene		8	16	calc. from Sutton et al., 1976	(Cano-Ruiz, et al., 1993)
polyethylene		70	8	calc. from Sutton et al., 1976	(Cano-Ruiz, et al., 1993)
polyethylene			9	Aged; calc. from Sabersky et al., 1975	(Cano-Ruiz, et al., 1993)
polyethylene			14	calc. from Altshuller and Wartburg, 1961	(Cano-Ruiz, et al., 1993)
polyethylene			4	calc. from Cohen et al., 1968	(Cano-Ruiz, et al., 1993)
paint on polyester	124	52	33		(Nicolas, et al., 2007)
paraffin wax	130	50-90	30		this study
beeswax	130	50-90	6		this study
dewaxed leaf					
cuticle	400	dry air		90 to 200	(Kerstiens and Lenzian, 1989)
tomato fruit cuticle	400	dry air	2		(Kerstiens and Lenzian, 1989)
tomato fruit cuticle	400	60	1		(Kerstiens and Lenzian, 1989)
spruce wood		0	20		(Grøntoft, et al., 2004)
spruce wood		30	25		(Grøntoft, et al., 2004)
spruce wood		50	10		(Grøntoft, et al., 2004)
spruce wood		70	6		(Grøntoft, et al., 2004)
spruce wood		90	2		(Grøntoft, et al., 2004)
spruce wood			14	for 'wet' surface	(Grøntoft, et al., 2004)
deionised water			29		(Grøntoft, et al., 2004)
moorland					
vegetation	30		0.2		(Fowler, et al., 2001)

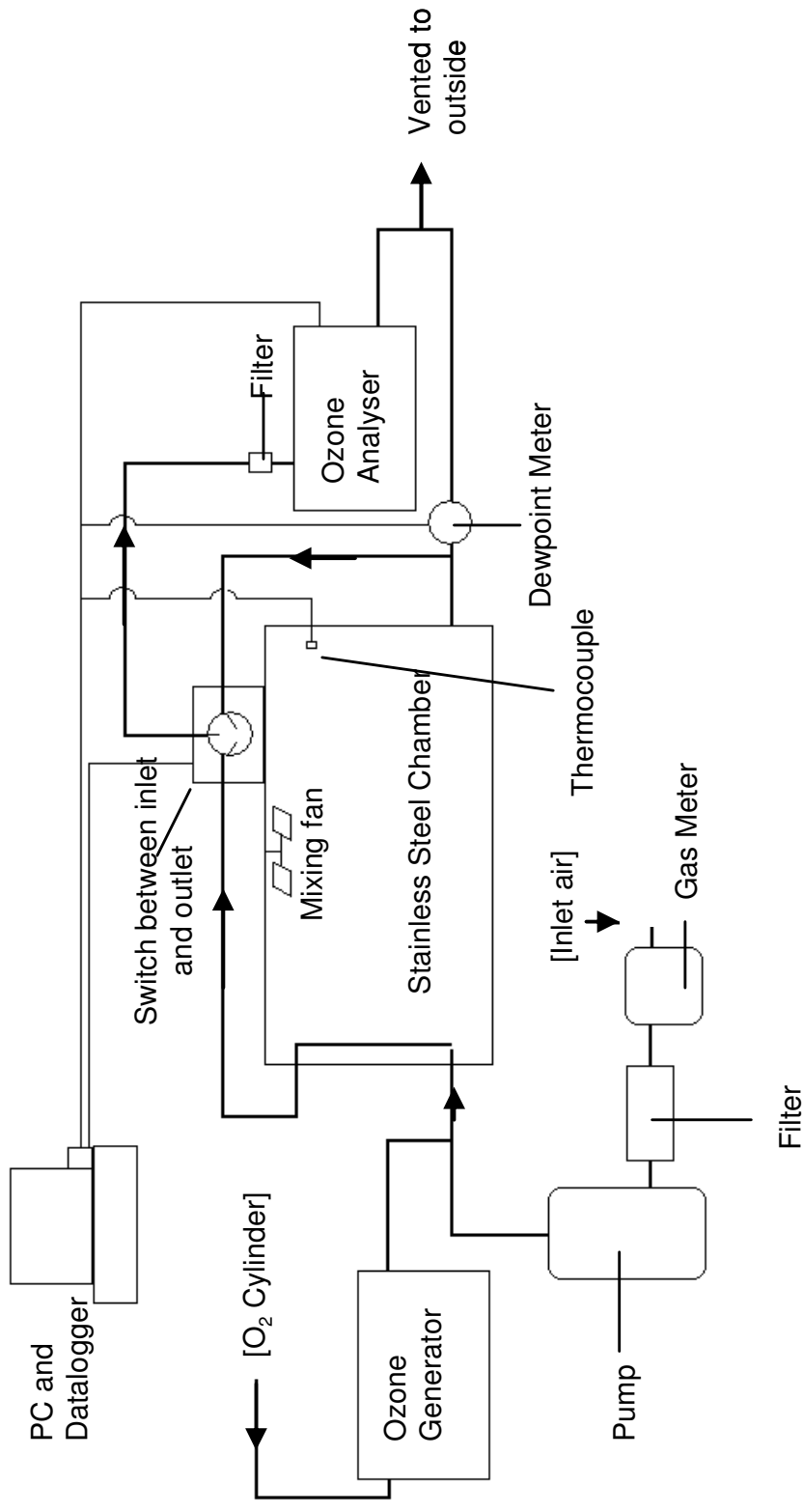


Figure 1. Schematic diagram of experimental system.

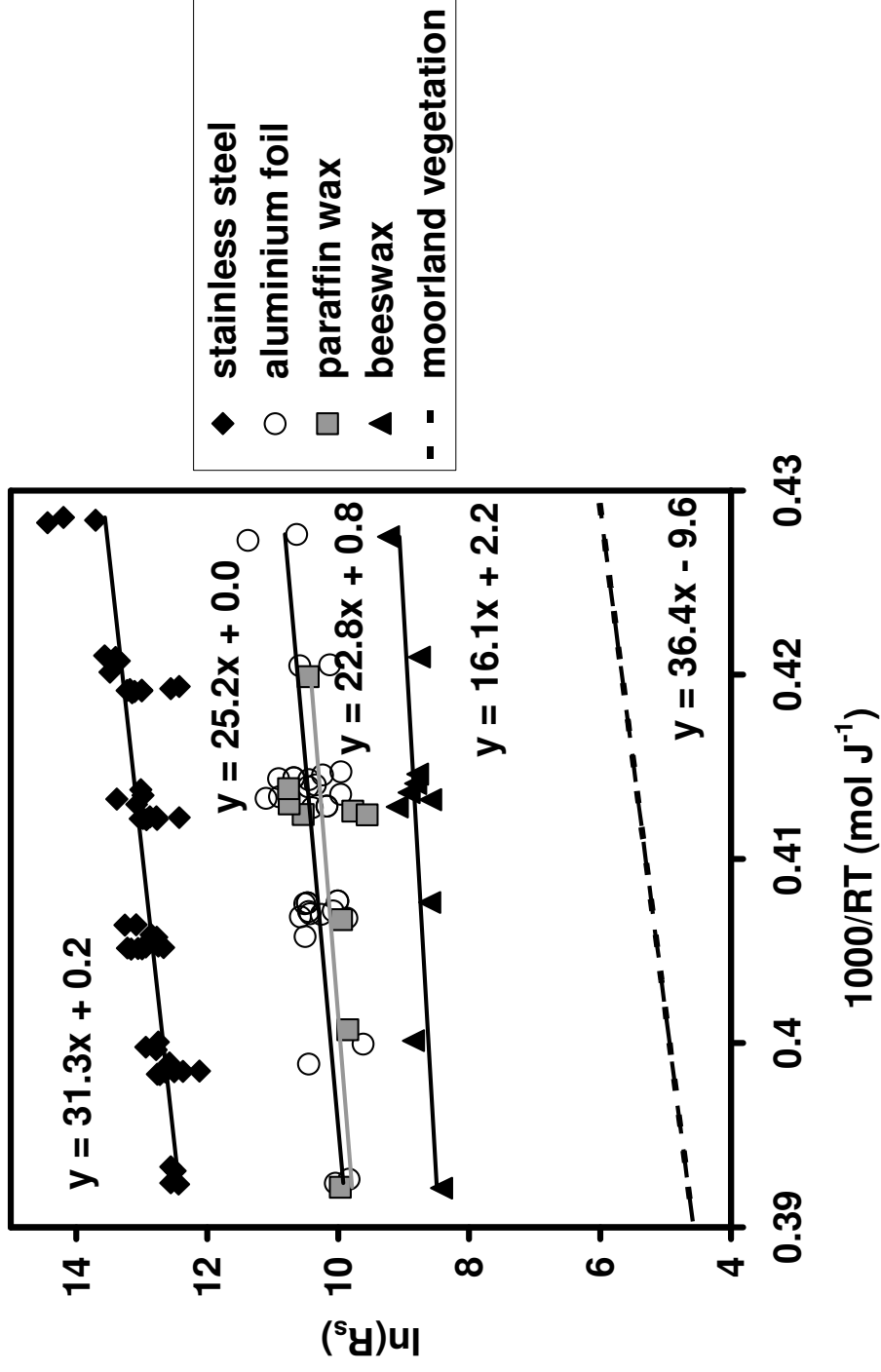


Figure 2. Dependence on temperature of O_3 removal rate at a range of surfaces, expressed as the natural logarithm (\ln) of the surface resistance (R_s). Each point represents a single experiment. The slope of the plot gives an apparent Arrhenius activation energy for the process. The line representing moorland vegetation is from long-term field measurements (Fowler et al., 2001).

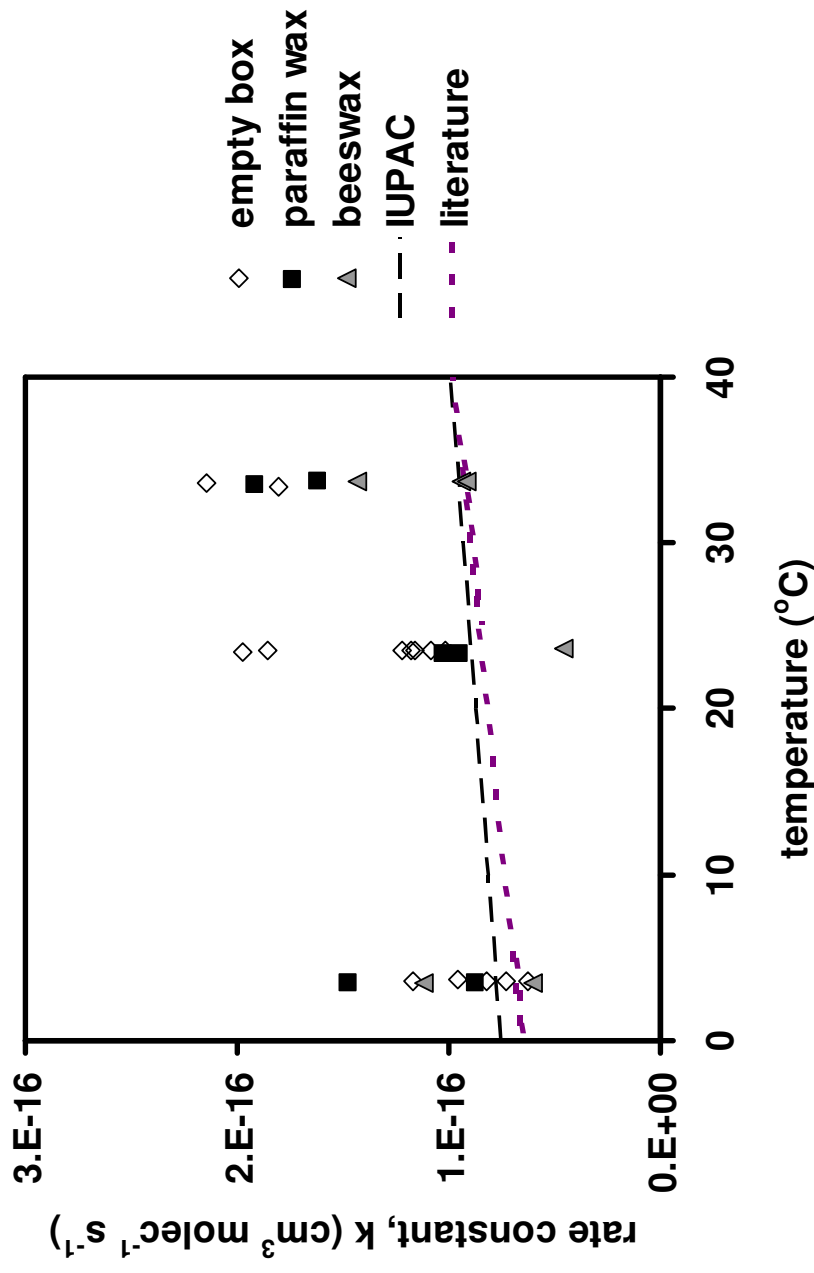


Figure 3. Calculated rate coefficient for the reaction of O₃ with α -pinene in the reaction chamber in the empty chamber (stainless steel walls) and in the presence of different wax surfaces, over a range of temperatures. Each point represents a single experiment. The recommended IUPAC rate coefficient for the homogeneous gas-phase reaction is shown (IUPAC, 2007), along with a recent literature value (Tillmann, et al., 2007).